

# Underwater sound of rigid-hulled inflatable boats

Christine Erbe,<sup>a)</sup> Syafrin Liong, Matthew Walter Koessler,  
Alec J. Duncan, and Tim Gourlay  
Centre for Marine Science & Technology, Curtin University, GPO Box U1987,  
Perth, WA 6845, Australia  
C.Erbe@curtin.edu.au, syafrin.liong@gmail.com,  
matthew.koessler@postgrad.curtin.edu.au, A.J.Duncan@curtin.edu.au,  
T.Gourlay@cmst.curtin.edu.au

**Abstract:** Underwater sound of rigid-hulled inflatable boats was recorded 142 times in total, over 3 sites: 2 in southern British Columbia, Canada, and 1 off Western Australia. Underwater sound peaked between 70 and 400 Hz, exhibiting strong tones in this frequency range related to engine and propeller rotation. Sound propagation models were applied to compute monopole source levels, with the source assumed 1 m below the sea surface. Broadband source levels (10–48 000 Hz) increased from 134 to 171 dB re 1  $\mu$ Pa @ 1 m with speed from 3 to 16 m/s (10–56 km/h). Source power spectral density percentile levels and 1/3 octave band levels are given for use in predictive modeling of underwater sound of these boats as part of environmental impact assessments.

© 2016 Acoustical Society of America  
[GBD]

Date Received: March 18, 2016 Date Accepted: June 6, 2016

## 1. Introduction

Concern about and research on bioacoustic impacts on marine mammals, fish, and other marine taxa is increasing.<sup>1</sup> Possible impacts include behavioral disturbance, acoustic masking, stress, shift in hearing sensitivity, and potentially more severe, long-term, or population-level effects.<sup>2,3</sup> Environmental impact assessments of marine operations often include the prediction of underwater sound from various operational scenarios that might involve rigid-hulled inflatable boats (RHIBs), also called rigid inflatable boats, and sometimes referred to by one of the brand names, “Zodiac™.” RHIBs are commonly used as support boats by marine and offshore industries, as patrol boats by coast guards, water police and military, as lifeboats in sea rescue, and as passenger vessels by whale-watching companies. These boats consist of rigid floorboards or hulls, with inflatable gunwales. RHIBs use outboard motors, typically single, but may have two or more for higher power.

To predict the sound levels received by marine fauna at some range (in the “far-field”), sound propagation models are used that mostly require monopole source levels as input. An underwater sound source near the sea surface radiates as a dipole formed by the point source and its surface-reflected image.<sup>4</sup> Sound propagation models that account for this surface-reflection require only the monopole source level as input. This is computed by recording the source in the far-field and applying a sound propagation model appropriate for the current and local environment, yielding the frequency-dependent propagation loss. In this article, we present monopole source spectra of RHIBs.

## 2. Methods

RHIBs (Fig. 1) were recorded at three sites: (1) Juan de Fuca Strait, outside of Victoria Harbour, British Columbia, Canada, (2) Haro Strait, British Columbia, Canada, and (3) Cockburn Sound, south of Perth, Western Australia (Table 1). In Canada, two omnidirectional hydrophones [International Transducer Corp. (CA, USA) 4123, bandwidth 50 Hz–25 kHz, sensitivity –145 dB re 1 V/ $\mu$ Pa] were lowered to depths of 5, 10, 15, or 25 m from a Canadian Coast Guard vessel that was drifting with the main engines switched off. Sound from both channels was pre-amplified, anti-aliased (high-frequency cutoff at 21 kHz), and recorded directly onto a PC hard drive (16 bit, sampling frequency 44.1 kHz/channel). RHIBs were identified using binoculars and a photo camera. The Coast Guard vessel’s radar yielded the distances to the RHIBs and their speeds. The speed was also measured with a police radar gun (Kustom Signals Inc., model Falcon 55E0483). Underwater sound recording began as soon as a RHIB approached and lasted 10–15 s. At site 1, RHIBs were passing at mostly 150–300 m, and were planing (traveling

<sup>a)</sup> Author to whom correspondence should be addressed.



Fig. 1. (Color online) Photo of the RHIB recorded in Western Australia.

at top speed). At site 2, RHIBs passed at low speeds, at distances of 10–60 m from the hydrophones. Conductivity-temperature-depth casts were done at both Canadian sites for sound propagation modeling. At site 3, in Australia, a Wildlife Acoustics Song Meter (Wildlife Acoustics Inc., MA, USA) SM2+ and hydrophone High Tech Inc.-92-WB (MS, USA) with built-in preamplifier (sensitivity  $-160$  dB re  $1$  V/ $\mu$ Pa, bandwidth 2 Hz–50 kHz, sampling frequency 96 kHz, 16 bit) in an underwater housing built by the Centre for Marine Science & Technology was deployed on the sandy seafloor in 8 m of water, and the GPS-tracked RHIB was driven close to the recorder at horizontal ranges of 7–18 m. Speed and engine rotations per minute (rpm; 1 rpm = 0.0167 rotations per second) were read off the RHIB’s GPS and tachometer, respectively. Ambient noise was recorded several times at each site for a few seconds in between vessel passes when no vessels were sighted within 2 km range.

All recordings were converted to sound pressure by applying the appropriate calibration factors, and these pressure values were then squared and smoothed over each recorded RHIB pass using a 1 s moving average. The 1 s segment with the highest mean square pressure was selected for further analysis and assumed to correspond to the closest point of approach (CPA). A spectrogram was calculated using 0.1 s Hann windows (hence 10 Hz resolution) with 50% overlap. The mean received spectrum for each RHIB pass was also computed. Monopole source spectra were calculated by adding the modeled propagation loss to the received spectrum levels,<sup>4</sup> using a parabolic equation model [RAMGeo (Ref. 5)] at sites 1 and 2, at the center frequencies of adjacent 1/3 octave bands from 50 Hz to 5 kHz, and a Gaussian beam tracing model [BELLHOP (Ref. 6)] from 6.3 to 20 kHz, with geoacoustic parameters taken from a local study.<sup>7</sup> Due to the close range of RHIB passes at site 3, a fast-field program [SCOOTER (Ref. 8)] was used with a seabed modeled as 2 m of sand<sup>9</sup> over a calcarenite halfspace.<sup>10</sup> The source depth was assumed to be 1 m.

Table 1. Summary of recordings of RHIBs. All RHIBs had outboard motors, in either single (1×) or twin (2×) configuration. At site 1, RHIBs were mostly passing in 12 m of water, and recordings were made on a drift into 70 m of water. At sites 2 and 3, water depth between source and recorder was constant. The RHIB at site 3 had a 4-stroke engine; the types of engine at sites 1 and 2 are unknown. Engine power is typically listed in units of hp on outboard motors; 1 hp = 745.7 W.

Site	Dates	Water depth [m]	# Recordings	Speed range [m/s (km/h)]	Outboard power [hp]	RHIB length [m]
1: Juan de Fuca Strait, CAN	1–4 Jun 1999	12–70	104	9–16 (32–56)	1 × 230; 2 × 150; 2 × 175; 2 × 225	7.0–9.1
2: Haro Strait, CAN	8–10 Jun 1999; 30 Aug 1999	70	12	3 (10–11)	1 × 230; 2 × 175; 2 × 225	7.0–9.1
3: Cockburn Sound, AUS	16 Oct 2015	8	26	4–11 (13–40)	1 × 90	6.5



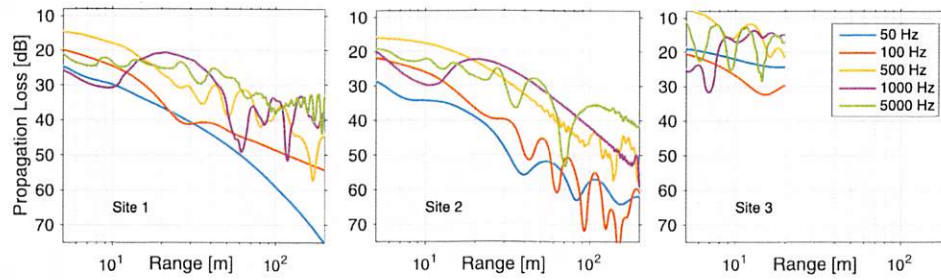


Fig. 2. (Color online) Propagation loss [dB] as a function of range at five frequencies. The modeled source depth was 1 m; the modeled receiver depth was 10 m in the examples shown for sites 1 and 2, and 8 m (resting on the seafloor) at site 3. Only short ranges (<20 m) were modeled at site 3.

### 3. Results

Modeled propagation loss showed a strong dependence on frequency, with poorer propagation of energy at lower frequencies in these shallow-water environments (Fig. 2). Median ambient noise was 104 dB re 1  $\mu$ Pa (50 Hz–21 kHz) at site 1, 101 dB re 1  $\mu$ Pa (50 Hz–21 kHz) at site 2, and 94 dB re 1  $\mu$ Pa (10 Hz–48 kHz) at site 3. The median signal-to-noise ratios at CPA were 18 dB (range 9–29 dB), 15 dB (range 8–29 dB), and 37 dB (range 33–41 dB), respectively.

The computed source spectra (power spectral density, PSD) are shown in Fig. 3 (left). PSD levels were highest at site 1, where RHIBs travelled the fastest, and lowest at site 2, where RHIBs travelled the slowest, with site 3 spectra and speeds in between. PSD percentile levels were computed over all recordings from all three sites (Fig. 3, right). The  $n$ th percentile gives the level that was exceeded  $n$ % of the time. The 50th percentile is the median. Table 2 lists the corresponding 1/3 octave band levels for use in sound propagation models requiring monopole source spectra.

All of the spectra exhibited strong tones between 70 and 400 Hz, likely relating to motor and propeller rotation. The RHIB at site 3 had a 4-cylinder, 4-stroke engine (Honda BF75-90), a propeller with 4 blades, and a gear ratio of 2.33:1. The propeller blade rate is the product of the number of blades and the propeller’s rotations per second. In terms of the engine rpm read off the tachometer, the propeller blade rate can be computed as  $4 \times \text{rpm}/2060/2.33$ . Figure 4 (left) shows the received spectrum from the RHIB at site 3 at 50 engine rotations per second (3000 rpm). The propeller blade rate and the engine firing rate are seen as tones with harmonics. Figure 4 (right) tracks the measured spectral peaks with engine rpm, in comparison to the expected propeller blade rate and the engine firing rate.

### 4. Discussion

Underwater sound from RHIBs was recorded at three sites. Recorded spectra were broadband and exhibited harmonically related tones corresponding to engine and propeller rotation. Overall, acoustic power increased with speed, in particular, at higher frequencies, likely related to increased propeller cavitation. At site 3, where only one RHIB was recorded, levels peaked at 6 m/s (20 km/h), which corresponds to its estimated “hump speed” of 15–20 km/h, at which it has a large bow-up trim angle, large resistance, and hence large loading on the propeller.

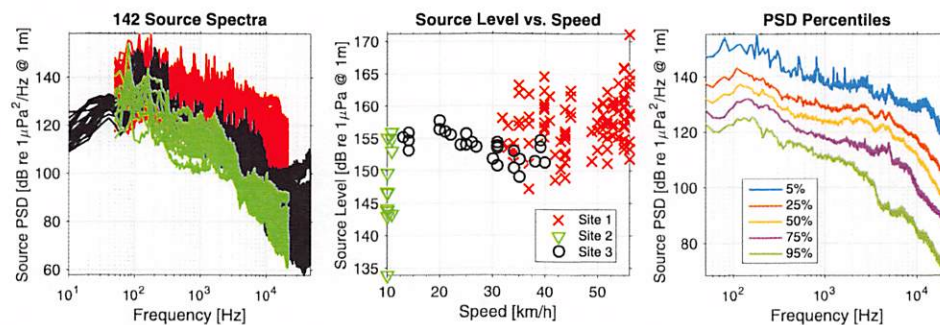


Fig. 3. (Color online) (Left) Source PSD of all 142 recordings at sites 1 (red), 2 (green), and 3 (black), shown over the respective system bandwidths. (Middle) Broadband source levels versus speed from all 142 passes. (Right) PSD percentile levels over all RHIB passes at all three sites.

Table 2. One-third octave source levels SL [dB re 1  $\mu$ Pa @ 1 m, source depth 1 m]: 5th, 25th, 50th (median), 75th, and 95th percentiles; fc: band center frequency.

fc/Hz	SL 5%/dB	SL 25%/dB	SL 50%/dB	SL 75%/dB	SL 95%/dB
50	135	136	140	146	156
63	132	137	143	149	160
80	135	139	146	153	165
100	137	143	149	155	164
125	139	146	152	157	165
160	140	147	151	156	167
200	138	146	151	156	168
250	138	147	151	155	165
315	135	145	148	153	165
400	136	143	148	153	161
500	136	142	147	153	165
630	136	142	147	153	162
800	135	142	148	153	164
1000	135	142	148	153	162
1250	135	141	148	153	163
1600	135	143	150	155	163
2000	135	143	151	155	164
2500	133	143	152	157	166
3150	131	142	151	156	164
4000	125	143	152	156	163
5000	123	144	152	156	165
6300	123	141	149	154	163
8000	122	140	148	153	163
10000	119	134	146	151	163
12500	117	131	142	149	165
16000	113	128	137	145	161

At the same speed, source levels differed by up to 20 dB. This variability is partly due to measurements of different RHIBs in three different environments, and uncertainty in the modeled hydro- and geoacoustic properties. RHIBs at sites 1 and 2 were not GPS tracked. The RHIB at site 3 was, however, the clock of the autonomous recorder drifted by a few seconds. We were therefore unable to determine the exact position of each RHIB at the time of strongest broadband received level, and instead assumed that this occurred at CPA. Vessels, however, have a frequency-dependent radiation pattern,<sup>11</sup> and the strongest level is not necessarily at CPA, leading to uncertainty and variability in reported source levels. Additional variability is due to the fact that at high speeds, RHIBs bounce on the water and the sound recorded underwater is modulated with the period of this bouncing (on the order of 1 s, depending on speed) leading to an alternating pattern of louder and quieter sections. At, e.g., 8.3 m/s

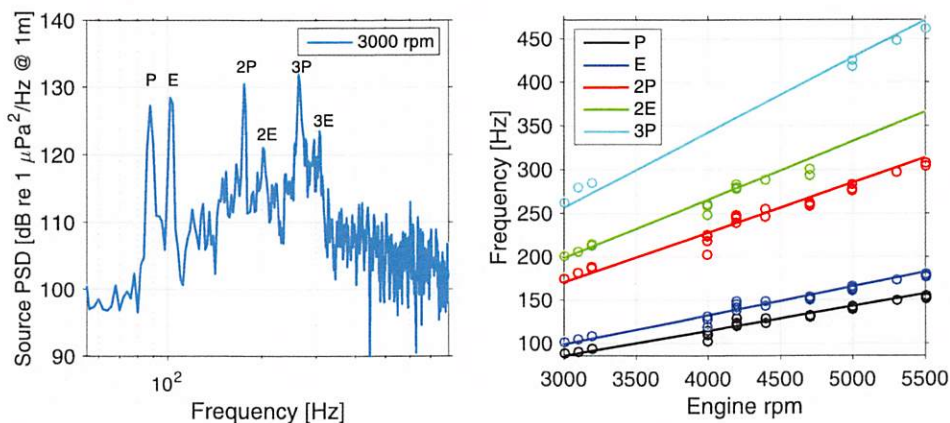


Fig. 4. (Color online) (Left) Received spectrum of the RHIB at site 3 at 3000 rpm of the engine, showing the propeller blade rate (P) and the engine firing rate (E), plus harmonics. (Right) Measured spectral peaks compared to the expected propeller blade rate and engine firing rate and harmonics at increasing engine rpm.



(30 km/h), a RHIB travels a significant distance within the 1 s recording used for analysis, in particular, at site 3, where recordings were made within a very short range. Yet another source of variability is the fact that engine rpm is not linearly related to speed; at constant rpm, the speed was up to 0.6 m/s (2 km/h) lower when the RHIB travelled against the wind.

The Canadian recordings were done opportunistically, with no control over speed or course, and missing information on engine type (2 or 4 stroke) and propeller blades. However, all of the Canadian RHIBs were longer and had more power than the Australian RHIB. At 8–11 m/s (30–40 km/h), where data from sites 1 and 3 overlap, it seems that the source levels of the longer and stronger RHIBs were mostly higher than those of the smaller Australian RHIB. Overall, the source level can be expected to vary with boat length, displacement, engine power, propeller number of blades, diameter, and pitch.

### Acknowledgments

The Canadian recordings were obtained while C.E. was part of David Farmer's group at the Institute of Ocean Sciences, Fisheries & Oceans Canada. C.E.'s former colleagues Kevin Bartlett, Frank Gerdes, Grace Kamitakahara-King, Roblyn Kendall, Ron Teichrob, Nick Hall-Patch, and Mark Trevorrow helped with instrumentation and fieldwork. Dave Minchin and Mal Perry helped with instrumentation in Australia. Sam Standish from Fremantle Sailing Club provided the RHIB and assistance with the Cockburn Sound measurements.

### References and links

- <sup>1</sup>R. Williams, A. J. Wright, E. Ashe, L. K. Blight, R. Bruintjes, R. Canessa, C. W. Clark, S. Cullis-Suzuki, D. T. Dakin, C. Erbe, P. S. Hammond, N. D. Merchant, P. D. O'Hara, J. Purser, A. N. Radford, S. D. Simpson, L. Thomas, and M. A. Wale, "Impacts of anthropogenic noise on marine life: Publication patterns, new discoveries, and future directions in research and management," *Ocean Coast. Manage.* **115**, 17–24 (2015).
- <sup>2</sup>A. N. Popper and T. Hawkins (eds.), *The Effects of Noise on Aquatic Life II. Advances in Experimental Medicine and Biology* (Springer Verlag, New York, 2016).
- <sup>3</sup>*The Effects of Noise on Aquatic Life. Advances in Experimental Medicine and Biology*, edited by T. Hawkins and A. N. Popper (Springer Verlag, New York, 2012).
- <sup>4</sup>M. Ainslie, *Principles of Sonar Performance Modelling* (Springer, New York, 2010).
- <sup>5</sup>M. D. Collins, "A split-step Padé solution for the parabolic equation method," *J. Acoust. Soc. Am.* **93**(4), 1736–1742 (1993).
- <sup>6</sup>M. B. Porter and H. P. Bucker, "Gaussian beam tracing for computing ocean acoustic fields," *J. Acoust. Soc. Am.* **82**(4), 1349–1359 (1987).
- <sup>7</sup>N. R. Chapman, L. Jaschke, M. A. McDonald, H. Schmidt, and M. Johnson, "Matched field geoacoustic tomography experiments using light bulb sound sources in the Haro Strait sea trial," in *IEEE Conference Proceedings Oceans'97*, October 6–9, 1997, pp. 763–768.
- <sup>8</sup>M. B. Porter, "The time-marched fast-field program (FFP) for modeling acoustic pulse propagation," *J. Acoust. Soc. Am.* **87**(5), 2013–2023 (1990).
- <sup>9</sup>E. L. Hamilton, "Geoacoustic modelling of the sea floor," *J. Acoust. Soc. Am.* **68**(5), 1313–1340 (1980).
- <sup>10</sup>A. Duncan, A. Gavrilov, and F. Li, "Acoustic propagation over limestone seabeds," in *Acoustics*, edited by A. C. Zander and C. Q. Howard (Australian Acoustical Society, Adelaide, Australia, 2009).
- <sup>11</sup>P. T. Arveson and D. J. Vendittis, "Radiated noise characteristics of a modern cargo ship," *J. Acoust. Soc. Am.* **107**(1), 118–129 (2000).